

# Femtosecond Laser Writing of PPV-Doped Three-Dimensional Polymeric Microstructures

Oriana Ines Avila , Nathália Beretta Tomazio, Adriano Jose Galvani Otuka, Josiani Cristina Stefanelo, Marcelo Barbosa Andrade, Debora Terezia Balogh, Cleber Renato Mendonca

São Carlos Institute of Physics, University of São Paulo, PO Box 369, São Carlos, SP 13560-970, Brazil

Correspondence to: C. R. Mendonca (E-mail: Crmendon@ifsc.usp.br)

Received 26 September 2017; accepted 1 December 2017; published online 10 January 2018

DOI: 10.1002/polb.24568

**ABSTRACT:** Poly(para-phenylene vinylene) (PPV) is a key material for optoelectronics because it combines the potential of both polymers and semiconductors. PPV has been synthesized via solution-processable precursor route, in which the precursor polymer poly(xylene tetrahydrothiophenium chloride) (PTHT) is thermally converted to PPV throughout the sample as a whole. Much effort has been devoted to fulfill spatial selectivity of PPV conversion. However, none of the methods proposed stand for PPV conversion three dimensionally, which would be appealing for the design of microdevices. Here, we demonstrate the potential of fs-laser direct writing via two-photon polymerization (2PP)

to fabricate PPV-doped 3D microstructures. PTHT is incorporated into the polymeric material and it is subsequently converted to PPV through a thermal treatment. Optical measurements, taken prior and after thermal conversion, confirm the PTHT to PPV conversion. Fs-laser direct writing via 2PP can be exploited to fabricate a variety of 3D microdevices, thus opening new avenues in polymer-based optoelectronics. © 2018 Wiley Periodicals, Inc. *J. Polym. Sci., Part B: Polym. Phys.* **2018**, *56*, 479–483

**KEYWORDS:** direct laser writing; electroluminescent polymers; femtosecond laser; PPV conversion; two-photon polymerization

**INTRODUCTION** Since researchers have found out a way to increase conductivity in polyacetylene<sup>1</sup> and have demonstrated poly(para-phenylene vinylene) (PPV) electroluminescence,<sup>2</sup> there has been a growing technological interest in conjugated polymers. These so-called organic semiconductors combine appealing optoelectronic properties of semiconductors with the ease of processing/shaping and low cost of polymers. In particular, PPV has a great potential for applications in electronic and luminescent devices<sup>3</sup> owing to its outstanding properties, such as electro- and photoluminescence<sup>2</sup> and electrical<sup>4</sup> and photoconductivity.<sup>5,6</sup> Though, like other highly conjugated materials, it exhibits poor solubility in organic solvents.<sup>7</sup>

To overcome this drawback, PPV is synthesized via a solution-processable precursor route, in which the precursor polymer, poly(xylene tetrahydrothiophenium chloride) (PTHT), is heated at temperatures on the order of 200 °C, resulting in a thermal conversion process to PPV by the elimination of tetrahydrothiophenium leaving groups,<sup>8,9</sup> as shown in Figure 1. Other conversion methods involve the irradiation with microwaves<sup>10</sup> or with UV light,<sup>11</sup> with the conversion given throughout the sample as a whole. Several strategies have been developed to allow PPV formation in specific regions of the sample including laser-induced elimination reactions in precursor polymer films under either UV

laser via one photon absorption<sup>12</sup> or fs-laser irradiation via two-photon absorption.<sup>13</sup> Also, 2D patterning of conjugated polymers may be achieved by direct laser writing<sup>14</sup> and e-beam lithography.<sup>15–17</sup> Nevertheless, these methods do not stand for 3D patterning of conjugated polymers, which would be interesting for the design of microdevices.

Fs-laser direct writing via two-photon polymerization (2PP) has become one of the most promising approaches for high-precision 3D microfabrication of organic materials.<sup>18–21</sup> This technique takes advantage of the spatial selectivity provided by two-photon absorption to fabricate microstructures with high definition and without geometrical limitation. Here, we exploit the potential of fs-laser direct writing via two-photon polymerization (2PP) to design 3D microstructures doped with the PPV precursor polymer PTHT, which is subsequently converted into PPV through a straightforward thermal treatment. Confocal fluorescence imaging and Raman, photoluminescence and absorption measurements were carried out to confirm the PTHT to PPV conversion.

## EXPERIMENTAL

### Fabrication of PPV-Doped Microstructures

Femtosecond laser-induced microfabrication was carried out using a negative-tone photoresist composed of two acrylic-

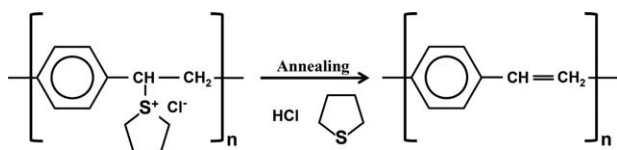


**FIGURE 1** Chemical structure of the precursor and the conversion process.

based monomers, a photoinitiator and PTHT (PPV precursor polymer). The monomers tris (2-hydroxy ethyl) isocyanurate triacrylate (SR368 – Sartomer<sup>®</sup>) and dipentaerythritol pentaacrylate (SR399 – Sartomer<sup>®</sup>) were mixed in a proportion of 10/90 wt%. This prepolymer resin has been used previously, with some differences in the monomers proportion, for photonic and biological applications.<sup>22–24</sup> Ethanol (2 mL) was added to the monomer composition to assist their dissolution. The PPV precursor, PTHT, was obtained from a water solution at a concentration of 1 mg/mL. It was synthesized according to the procedure described elsewhere.<sup>25</sup> In brief, using a Schlenk type reactor in inert atmosphere, 7 mL of a 0.4 M aqueous sodium hydroxide solution was added dropwise to 1 g of *p*-xylylenebis(tetrahydrothiophenium chloride) dissolved in 10 mL of methanol under magnetic stirring. After 20 min, 7 mL of 0.4 M aqueous hydrochloric acid was added dropwise to the reaction. The resulting polymer solution was purified by dialysis. The final concentration was adjusted with ultrapure water to 1 mg/mL. An aliquot of this solution was added to the acrylic monomers, resulting in a proportion of PTHT of 0.5 wt% (chosen to allow a homogenous resin composition). After the mixture had been stirred for 2 h at 30 °C, it was kept in vacuum at 30 °C for 3 days. Once the solvent had been evaporated, the photoinitiator 2,4,6-trimethylbenzoylphenyl phosphinate (Lucirin TPO-L – Igarcure<sup>®</sup>),<sup>26,27</sup> the compound responsible for triggering polymerization when excited via two-photon absorption, was added to the polymeric resin in a proportion of 3 wt% based on total resin. The photoresist was deposited onto a glass substrate, covered by a coverslip with a spacer and placed on a motorized stage mounted on an inverted microscope. The polymerization was driven by focusing 100-fs pulses of a mode-locked Ti:Sapphire oscillator operating at 780 nm (86 MHz) into the photoresist using a NA 0.85 objective lens. By scanning the laser three dimensionally with the help of a galvanometric-mirror system along with the motorized stage that supports the photoresist, the microstructures are fabricated. Further details regarding the microfabrication process are provided elsewhere.<sup>21,28</sup> After the fabrication step had been finished, the microstructures were heated in a vacuum oven at 230 °C/6 h to induce the thermal conversion of PTHT to PPV.

### Microstructure Characterization

The microstructures fabricated via femtosecond laser-induced two-photon polymerization (2PP) were characterized by scanning electron (Hitachi TM3000<sup>®</sup>) and z-stack confocal fluorescence microscopies (Zeiss LSM 700<sup>®</sup>, 40× Objective lens, excitation at 445 nm, 1 μm of z-step).

Their optical properties, prior and after the thermal conversion process, were analyzed through micro-photoluminescence and -absorption setups assembled on an inverted microscope. The excitation source (HeCd laser at 442 nm) is brought to the sample through the entrance port of the microscope and focused by a NA 0.25 objective lens. The microstructures fluorescence was collected by positioning an optical fiber in the proximity of the microstructures with the aid of a micromanipulator, while the other end of the fiber was connected to a spectrometer (*Ocean Optics USB2000f*<sup>®</sup>). Their absorption spectrum, in the UV–vis range, was obtained through a similar setup, replacing the HeCd laser by a halogen lamp/violet led/blue led as illumination source. Raman measurements were performed at room temperature with a LabRam HR Evolution Raman spectrometer, using a laser of wavelength 532 nm as excitation source and a Peltier-cooled CCD detector.

### RESULTS AND DISCUSSION

Figure 2(a) shows scanning electron microscopy images of three-dimensional microstructures fabricated by employing 50 pJ pulses from the Ti:Sapphire laser oscillator with 40 μm/s of laser beam scanning speed. As can be inferred from the scanning electron micrographs, they exhibit good structural integrity and low shrinkage despite the presence of the PTHT (PPV precursor), which is readily integrated into the polymer host material.

After the microstructures had undergone thermal conversion (described in the Experimental section), the PPV spatial distribution was analyzed by confocal fluorescence microscopy. The reconstructed fluorescence micrographs illustrated in Figure 2(b) reproduce the scanning electron micrograph geometry, thus confirming that the femtosecond laser writing process does not affect PPV optical properties and it is uniformly distributed throughout the microstructures. The height mismatch between both micrographs is attributed to a measurement artifact. As the excitation and detection of the confocal fluorescence microscope are given from above, fluorescence is re-absorbed by the PPV molecules present in the microstructure close-to-top layers until it hits the detector. Wherefore, for an integration time set to avert signal saturation from the close-to-top layers, fluorescence from shorter layers is barely detected.

To verify both, the presence of PTHT and its conversion to PPV into the microstructure, micro-photoluminescence and -absorption were carried out. Given the micrometric dimensions of such structures, their absorption/luminescence spectra could not be acquired by means of standard spectrometers, which require macroscopic samples. The fluorescence spectra of the microstructures doped with PTHT, prior and after thermal conversion, are presented in Figure 3. The fluorescence spectrum of PTHT-doped microstructures exhibits a band with a peak centered at 490 nm and shoulders at 515 and 560 nm. After thermal conversion, a red shift is observed in the fluorescence spectrum due to an increase in the conjugation degree of the polymer. There are peaks

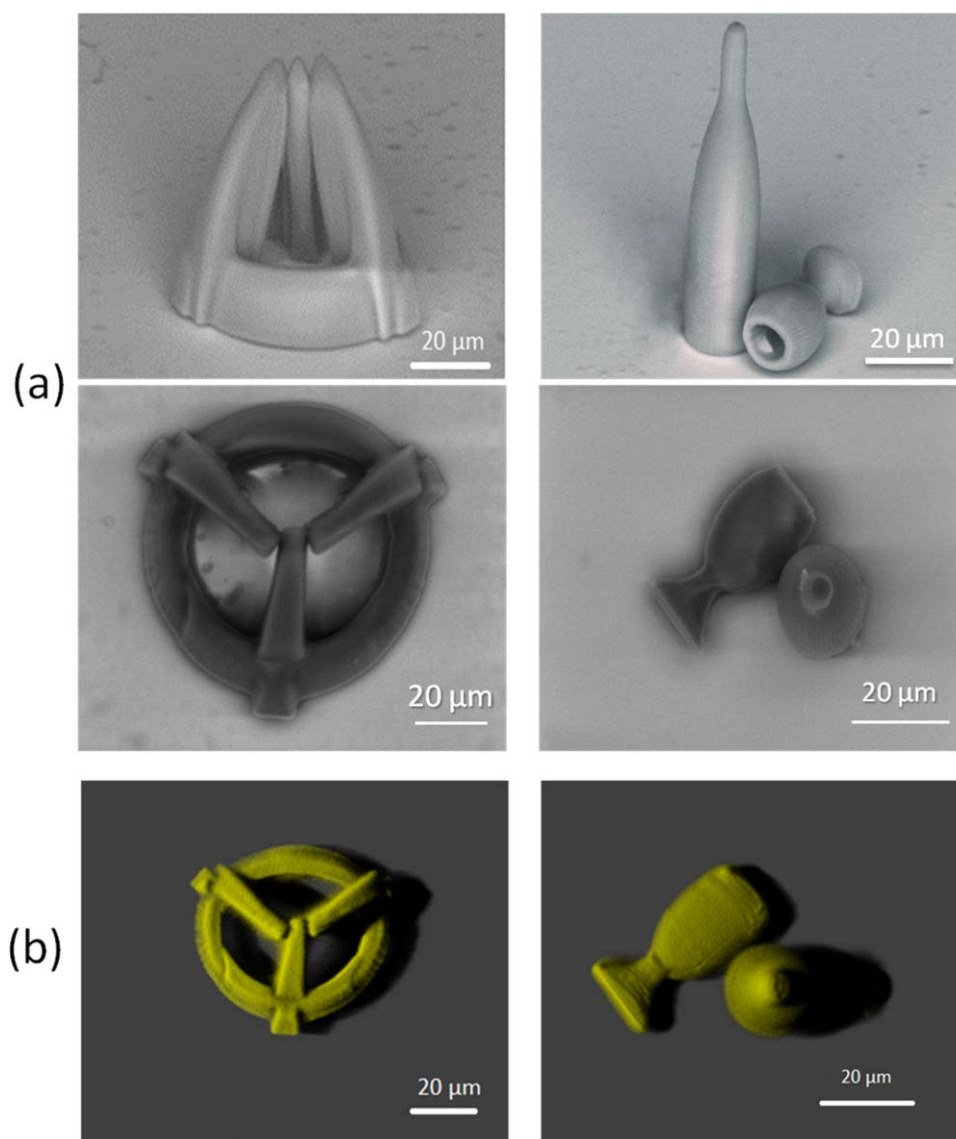


**FIGURE 2** (a) Scanning electron and (b) 3D reconstructed confocal fluorescence micrographs of PPV-doped microstructures produced by two-photon polymerization. [Color figure can be viewed at [wileyonlinelibrary.com](http://wileyonlinelibrary.com)]

centered at 515 and 550 nm and a small shoulder around 600 nm, which are characteristic of PPV. It is worth mentioning that, even though the photoinitiator Lucirin TPO-L is present at a concentration 6 times higher in wt% than the polymer precursor, it does not contribute to the emission spectra of the microstructures either prior or after the thermal conversion. The excitation of the microstructures in the micro-luminescence setup was carried out at 442 nm, which is out of the absorption spectrum of Lucirin TPO-L.<sup>26</sup> As shown in the optical microscopy images presented as insets in Figure 3, the microstructure doped with the precursor polymer (left image) exhibits a slightly greenish color, typical of PTHT. The microstructures thermally converted, however, present an evident color change to yellow, typical of PPV.

As a complementary analysis, absorption measurements of the PPV-doped microstructures were performed (after heat

treatment). The absorption spectrum presented in Figure 4 features a broad band extending from 430 nm to 520 nm, with a maximum close to 460 nm. PPV absorption bands within 300–420 nm are out of the spectrum range that we are able to measure with our micro-absorption setup and, therefore, are not shown in Figure 4. The conversion of PTHT into PPV is accompanied by the reduction of absorption bands in the UV region (~200 to 270 nm, not displayed herein) attributed to the elimination of tetrahydrothiophenium units. The appearance of new bands around 470 nm is related to the formation of conjugated PPV segments of different sizes.<sup>8,9,29–31</sup> Again, there are no spectral characteristics of Lucirin TPO-L in the absorption spectra shown herein. Our micro-absorption setup comprises light sources from 430 nm upward higher wavelengths, which is out of the absorption spectrum of Lucirin TPO-L.

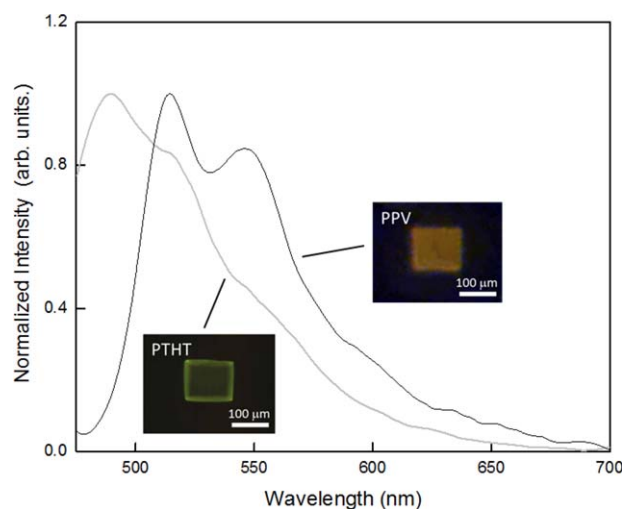


**FIGURE 3** Photoluminescence (PL) spectra of a microstructure doped with PTHT (gray line) and the same microstructure after thermal conversion to PPV (black line). The fluorescence spectra were normalized to the higher energy peak. The inset displays images of the microstructures being excited with a HeCd laser at 442 nm before (left) and after (right) thermal conversion. [Color figure can be viewed at [wileyonlinelibrary.com](http://wileyonlinelibrary.com)]

Figure 5 displays the Raman spectrum of the microstructure after thermal conversion to PPV (black line). It shows the typical PPV peaks,<sup>32–34</sup> with the most important ones centered at 1328 and 1628  $\text{cm}^{-1}$ , which correspond to the double bond stretching vibration of the vinyl group. The other peaks (at 966, 1170, 1302, 1547, and 1584  $\text{cm}^{-1}$ ) are characteristic of the molecule aromatic ring. The vibrations at 1414  $\text{cm}^{-1}$  are assigned to deformation vibrations of  $\text{CH}_2$  (present in PPV and acrylic materials) and the peaks at 1455  $\text{cm}^{-1}$  and 1726  $\text{cm}^{-1}$  stand for the photoinitiator aromatic rings and the carbonyl group of acrylic materials, respectively.<sup>35</sup> For comparison purposes, the gray line in

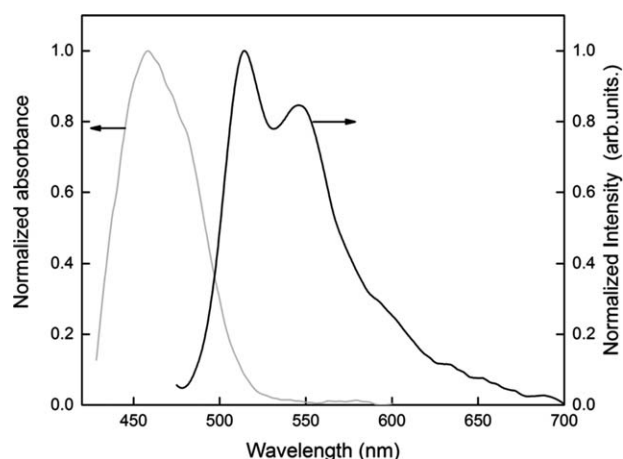


**FIGURE 4** Linear absorption (gray line) and photoluminescence (PL) spectra (black line) of a microstructure after thermal conversion to PPV. The spectra were normalized to the higher energy peak.

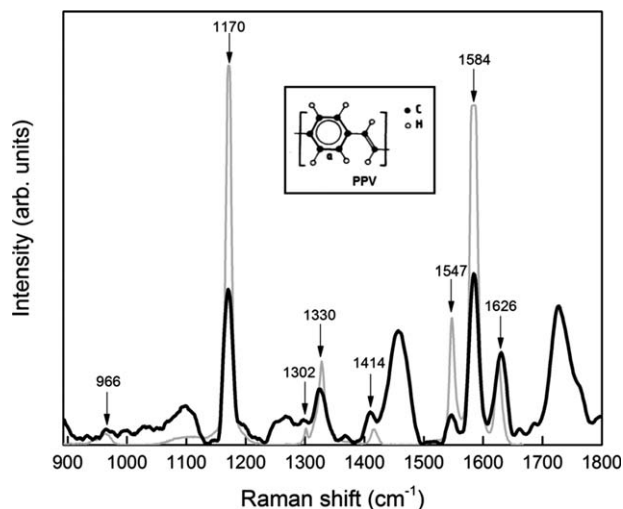


**FIGURE 5** PPV Raman spectra recorded under excitation at 532 nm. The black line refers to the microstructure after thermal conversion to PPV, while its gray counterpart stands for a PPV film thermally converted at 230 °C for 6 h. The Raman spectrum of the microstructure was multiplied by a factor of 10.

Figure 5 displays the Raman spectrum of a PPV film converted from a only PTHT film through the same thermal treatment.

## CONCLUSIONS

PPV-doped 3D microstructures were successfully fabricated by means of fs-laser direct writing via two-photon polymerization. After fabrication, the microstructures were submitted to a standard thermal treatment for converting PTHT into PPV. The scanning electron micrographs display microstructures featuring good structural quality and low shrinkage despite the presence of the dopant. Besides, there was a good match in geometry between the reconstructed fluorescence and scanning electron micrographs taken after thermal treatment, thereby confirming that PPV is uniformly distributed throughout the microstructures.

To measure the optical properties of PPV incorporated into the microstructures, micro-photoluminescence, and absorption setups were assembled. The results showed a red shift in the microstructure fluorescence spectrum after thermal conversion, which is attributed to an increase in the conjugation degree of the polymer. Images of the microstructures being excited with a HeCd laser at 442 nm revealed an evident color change of the microstructure fluorescence to yellow, typical of PPV. In addition, PPV peaks showed up in the microstructure absorption and Raman spectra, thereby confirming the presence of PPV in the microstructure after thermal conversion.

## ACKNOWLEDGMENTS

The authors gratefully acknowledge financial support from CNPq, FAPESP (2011/12399-0, 2013/20884-0, 2013/03487-

8, and 2016/20094-8) and CAPES. They also would like to thank Sartomer and Arkema Brazil for donating the acrylic monomers SR399 and SR368.

#### REFERENCES AND NOTES

- 1 C. K. Chiang, C. R. Fincher, Y. W. Park, A. J. Heeger, H. Shirakawa, E. J. Louis, S. C. Gau, A. G. Macdiarmid, *Phys. Rev. Lett.* **1977**, *39*, 1098.
- 2 J. H. Burroughes, D. D. C. Bradley, A. R. Brown, R. N. Marks, K. Mackay, R. H. Friend, P. L. Burn, A. B. Holmes, *Nature* **1990**, *347*, 539.
- 3 L. J. Rothberg, A. J. Lovinger, *J. Mater. Res.* **1996**, *11*, 3174.
- 4 I. Murase, T. Ohnishi, T. Noguchi, M. Hirooka, *Synth. Met.* **1987**, *17*, 639.
- 5 H. Antoniadis, B. R. Hsieh, M. A. Abkowitz, S. A. Jenekhe, M. Stolka, *Synth. Met.* **1994**, *62*, 265.
- 6 U. Rauscher, H. Bässler, D. D. C. Bradley, M. Hennecke, *Phys. Rev. B* **1990**, *42*, 9830.
- 7 L. Akcelrud, *Prog. Polym. Sci.* **2003**, *28*, 875.
- 8 T. Junkers, J. Vandenbergh, P. Adriaensens, L. Lutsen, D. Vanderzande, *Polym. Chem.* **2012**, *3*, 275.
- 9 D. D. C. Bradley, *J. Phys. D: Appl. Phys.* **1987**, *20*, 1389.
- 10 A. Torres, R. W. Lenz, *J. Appl. Polym. Sci.* **1994**, *52*, 377.
- 11 J. Wery, B. Dulieu, E. Launay, J. Bullot, M. Baitoul, J. P. Buisson, *Synth. Met.* **1997**, *84*, 277.
- 12 S. Y. Paik, S. H. Kwon, O. J. Kwon, J. S. Yoo, M. K. Han, *Synth. Met.* **2002**, *129*, 101.
- 13 O. I. Avila, J. M. P. Almeida, F. R. Henrique, R. D. Fonseca, G. F. B. Almeida, D. T. Balogh, C. R. Mendonca, *J. Mater. Chem. C* **2017**.
- 14 A. J. C. Kuehne, D. Elfström, A. R. Mackintosh, A. L. Kanibolotsky, B. Guilhabert, E. Gu, I. F. Perepichka, P. J. Skabara, M. D. Dawson, R. A. Pethrick, *Adv. Mater.* **2009**, *21*, 781.
- 15 B. S. Holdcroft, *Adv. Mater.* **2001**, *13*, 1753.
- 16 S. H. M. Persson, P. Dyreklev, O. Inganäs, *Adv. Mater.* **1996**, *8*, 405.
- 17 M. Angelopoulos, N. Patel, J. M. Shaw, N. C. Labianca, S. A. Rishton, *J. Vac. Sci. Technol. B Microelectron. Nanom. Struct. Process. Meas. Phenom.* **1993**, *11*, 2794.
- 18 R. Guo, S. Xiao, X. Zhai, J. Li, A. Xia, W. Huang, *Opt. Express*, **2006**, *14*, 810.
- 19 K. K. Seet, V. Mizeikis, S. Matsuo, S. Juodkazis, H. Misawa, *Adv. Mater.* **2005**, *17*, 541.
- 20 Z.-P. Liu, Y. Li, Y.-F. Xiao, B.-B. Li, X.-F. Jiang, Y. Qin, X.-B. Feng, H. Yang, Q. Gong, *Appl. Phys. Lett.* **2010**, *97*, 211105.
- 21 N. B. Tomazio, A. J. G. Otuka, G. F. B. Almeida, X. Roselló-Mechó, M. V. Andrés, C. R. Mendonça, *J. Polym. Sci. B: Polym. Phys.* **2017**, *55*, 569.
- 22 N. Li, M. Driscoll, G. Kumi, R. Hernandez, K. J. Gaskell, W. Losert, J. T. Fourkas, *J. Am. Chem. Soc.* **2008**, *130*, 13512.
- 23 L. Li, E. Gershgoren, G. Kumi, W. Y. Chen, P. T. Ho, W. N. Herman, J. T. Fourkas, *Adv. Mater.* **2008**, *20*, 3668.
- 24 D. S. Correa, P. Tayalia, G. Cosendey, D. S. Dos Santos, R. F. Aroca, E. Mazur, C. R. Mendonca, *J. Nanosci. Nanotechnol.* **2009**, *9*, 5845.
- 25 J. B. Schlenoff, L. Wang, *J. Macromol.* **1991**, *24*, 6653.
- 26 C. R. Mendonca, D. S. Correa, T. Baldacchini, P. Tayalia, E. Mazur, *Appl. Phys. A: Mater. Sci. Process.* **2008**, *90*, 633.
- 27 T. Baldacchini, C. N. LaFratta, R. A. Farrer, M. C. Teich, B. E. A. Saleh, M. J. Naughton, J. T. Fourkas, *J. Appl. Phys.* **2004**, *95*, 6072.
- 28 D. S. Correa, M. R. Cardoso, V. Tribuzi, L. Misoguti, C. R. Mendonca, *IEEE J. Sel. Top. Quantum Electron.* **2012**, *18*, 176.
- 29 J. Obrzut, F. E. Karasz, *J. Chem. Phys.* **1987**, *87*, 2349.
- 30 M. Herold, J. Gmeiner, W. Rieß, M. Schwoerer, *Synth. Met.* **1996**, *76*, 109.
- 31 J. Wery, B. Dulieu, J. Bullot, M. Baitoul, P. Deniard, J.-P. Buisson, *Polymer (Guildf)* **1999**, *40*, 519.
- 32 A. Sakamoto, Y. Furukawa, M. Tasumi, *J. Phys. Chem.* **1992**, *96*, 1490.
- 33 D. Rakovic, R. Kostic, L. A. Gribov, I. E. Davidova, *Phys. Rev. B* **1990**, *41*, 10744.
- 34 S. Lefrant, E. Perrin, J. P. Buisson, H. Eckhardt, C. C. Han, *Synth. Met.* **1989**, *29*, E91.
- 35 E. Smith, G. Dent, *Modern Raman Spectroscopy – A Practical Approach*; Wiley: New York, **2005**.